

A phase diagram for jammed matter

Chaoming Song¹, Ping Wang¹ & Hernán A. Makse^{1,2}

The problem of finding the most efficient way to pack spheres has a long history, dating back to the crystalline arrays conjectured¹ by Kepler and the random geometries explored² by Bernal. Apart from its mathematical interest, the problem has practical relevance³ in a wide range of fields, from granular processing to fruit packing. There are currently numerous experiments showing that the loosest way to pack spheres (random loose packing) gives a density of ~55 per cent^{4–6}. On the other hand, the most compact way to pack spheres (random close packing) results in a maximum density of ~64 per cent^{2,4,6}. Although these values seem to be robust, there is as yet no physical interpretation for them. Here we present a statistical description of jammed states⁷ in which random close packing can be interpreted as the ground state of the ensemble of jammed matter. Our approach demonstrates that random packings of hard spheres in three dimensions cannot exceed a density limit of ~63.4 per cent. We construct a phase diagram that provides a unified view of the hard-sphere packing problem and illuminates various data, including the random-loose-packed state.

Difficulties in describing static granular materials and other jammed systems, such as compressed emulsions, stem from the lack of well-defined conservation laws on which a statistical description of the system can be based. Unlike in equilibrium statistical mechanics, energy no longer describes the microstates of the system, owing to the dissipative and athermal nature of jammed matter. Thus, many experimental and theoretical studies focus on the analysis of the system volume as the analogue of system energy in equilibrium thermal systems^{7–16}. Recent advances in X-ray tomography¹³ and confocal microscopy¹⁷ have revealed the detailed internal structure of jammed matter, allowing for the study of the free volume per particle, or free volume function, denoted W (ref. 7). By partitioning the space into a set of non-overlapping volumes with Voronoi diagrams, these studies show that W is distributed with exponential tails^{13,14,17}. More importantly, experiments with monodisperse hard spheres¹³ show that W is inversely proportional to the coordination number (number of contacts) of the particle, z .

From a theoretical perspective, the study of the ensemble of jammed matter requires an analytical form for W (refs 7, 9, 10, 15). We first derive the Voronoi volume in terms of the particle positions (see Supplementary Information section IA) and then use statistical analysis to coarse-grain the Voronoi volume over a mesoscopic length scale, obtaining a mesoscopic free volume function (see Supplementary Information section IB) that is analytically tractable. For monodisperse hard spheres (grains) of volume V_g , we find:

$$W(z) = \frac{2\sqrt{3}}{z} V_g \quad (1)$$

The inverse relation with z is in general agreement with experiments¹³. The calculation of $W(z)$ is based on the environment of the grains, where each particle is assumed to be in a uniform background field produced by the other particles and not influenced by the

particle. Thus, equation (1) is akin to a quasi-particle theory: the coordination number z in equation (1) can be considered a coarse-grained average associated with ‘quasi-particles’ with free volume W . The key result is the relation between the Voronoi volume and the coordination number. This makes it possible to incorporate the volume function into a statistical mechanical description in terms of jammed hard spheres, using the constraint of mechanical stability as we show below.

The canonical partition function in the volume ensemble is the starting point for the statistical mechanics of jamming⁷, where the role traditionally played by the energy in thermal systems is replaced by the volume:

$$Q(X) = \int g(W) e^{-W/X} \Theta_W dW \quad (2)$$

Here X is the compactivity in units of volume⁷, determining the macrostates of the system (see below for an interpretation of this temperature-like parameter); $g(W)$ is the density of jammed states for a given volume W ; and Θ_W formally imposes the condition of jamming on the ensemble through force and torque balance. The main components of the theory are the uniformity assumptions behind the calculation of the mesoscopic volume function (see Supplementary Information section IC), the identification of the isostatic condition with the ensemble of jammed configurations, and the derivation of the density of states, as we discuss below.

Distinguishing between metastable and mechanically stable packings that define the jammed state through the Θ_W function is an unsolved problem¹⁸, and is related to the more fundamental question of whether or not a jammed packing is well defined. In practice, it is widely believed that the isostatic condition is necessary for a jammed disordered packing^{19–23}. That is, the number of force variables in the system is equal to the number of force and torque balance equations (see Supplementary Information section II). Therefore, we assume that the Θ_W function in equation (2) restricts the ensemble to the isostatic packings.

It is important to note that the coordination number z , as defined in equation (1), refers to the geometry of the packing and does not refer to contact forces. Therefore, z can include ‘trivial’ contacts with zero force, not contributing to the mechanical balance. We call z the geometrical coordination number to distinguish it from the mechanical coordination number Z , which is less than or equal to z and includes the contacts with non-zero force (see Supplementary Information section III). The mechanical coordination number thus directly corresponds to the isostatic condition of force and torque balance. For frictionless spherical particles (with interparticle friction coefficient $\mu = 0$, mimicking emulsion systems), the isostatic condition implies that $Z = 2d = 6$ (d is the dimension of the system, and in the following $d = 3$). For infinitely rough particles with $\mu \rightarrow \infty$, the mechanical coordination number is $Z = d + 1 = 4$ (see Supplementary Information section II for details). Interpolating between these two limits there must exist granular packings of finite

¹Levich Institute and Physics Department, City College of New York, New York, New York 10031, USA. ²Departamento de Física, Universidade Federal do Ceará, 60451-970 Fortaleza, Ceará, Brazil.

μ with $Z(\mu)$ smoothly varying between $Z(\mu = 0) = 6$ and $Z(\mu \rightarrow \infty) = 4$ (ref. 23). This is an important assumption that we test by numerical simulation (see Supplementary Information section II), where we find a common $Z(\mu)$ curve (Supplementary Fig. 10) for different packing preparation protocols. The mechanical coordination number ranges from four to six as a function of μ , and provides a lower bound on the geometrical coordination number: $Z \leq z \leq 6$. These bounds are tested in computer simulations in Supplementary Information section IIIA.

By changing variables, we can write equation (2) as (see Supplementary Information section IV):

$$Q_{\text{iso}}(X, Z) = \int_Z^6 e^{-W(z)/X} g(z) dz \quad (3)$$

Owing to the implicit volume coarse-graining in equation (1), each volume state $W(z)$ represents a mesoscopic state containing many microstates with a common value of z and density of states $g(z)$. The latter can be calculated as follows (see Supplementary Information section IV). We assume that the hard spheres are packed in a collectively jammed configuration in which no motion of any subset of particles can lead to unjamming²⁴. Thus, the configuration space of jammed matter is discrete, as we cannot continuously change one configuration to another. We denote the dimension per particle of the configuration space by \mathcal{D} and assume that the distance between two configurations is not broadly distributed, with a mean distance h_z . Therefore, the number of configurations is proportional to $1/(h_z)^{\mathcal{D}}$, analogous with that in quantum mechanics, h^{-d} , where h is Planck's constant and d is the dimension. The fact that the particles are jammed by z contacting particles reduces the number of degrees of freedom to $\mathcal{D} - z$, and the number of configurations is then $1/(h_z)^{\mathcal{D}-z}$. Because the term $1/(h_z)^{\mathcal{D}}$ is a constant, it will not influence the average in the partition function. Therefore, we have $g(z) = (h_z)^z$.

From equation (3) we obtain the equations of state that define the phase diagram of jamming. We start by investigating two limiting cases (see Supplementary Information section V). First, in the limit of vanishing compactivity ($X \rightarrow 0$), we obtain the ground state of jammed matter with a density

$$\phi_{\text{RCP}} = \frac{6}{6+2\sqrt{3}} \approx 0.634 \quad (4)$$

for $Z(\mu) \in [4, 6]$. Second, in the limit of infinite compactivity ($X \rightarrow \infty$), we obtain

$$\begin{aligned} \phi_{\text{RLP}}(Z) &= \frac{1}{Q_{\text{iso}}(\infty, Z)} \int_Z^6 \frac{z}{z+2\sqrt{3}} (h_z)^z dz \\ &\approx \frac{Z}{Z+2\sqrt{3}} \end{aligned} \quad (5)$$

for $Z(\mu) \in [4, 6]$.

The average in equation (5) is taken over all states with equal probability, because $e^{-W(z)/X} \rightarrow 1$ as $X \rightarrow \infty$, and the approximation applies because h_z is very small and the most populated state, $z = Z$, thus makes the dominant contribution to the average volume. The meaning of the subscripts 'RCP' (random close packing) and 'RLP' (random loose packing) in equations (4) and (5) will become clear below.

The equations of state (4) and (5) are plotted in the ϕ - Z plane in Fig. 1, illustrating the phase diagram of jammed matter. The phase space is limited to lie above the line of minimum coordination number, $Z = 4$ (for infinitely rough grains), labelled 'granular line' in Fig. 1. All mechanically stable, disordered jammed packings lie within the confining limits of the phase diagram (Fig. 1, yellow zone), and are forbidden in the grey area. For example, a packing of frictional hard spheres with $Z = 5$ (corresponding to a granular material with interparticle friction coefficient $\mu \approx 0.2$, according to Supplementary Fig. 10) cannot be equilibrated at volume fractions below

$\phi < \phi_{\text{RLP}}(Z = 5) = 5/(5+2\sqrt{3}) = 0.591$ or above $\phi > \phi_{\text{RCP}} = 0.634$. Thus, these results provide a statistical interpretation of the RLP and RCP limits, as follows.

First, originating in the statistical mechanics approach, the RCP limit arises as the result of equation (4), which gives the maximum volume fraction of disordered packings. The RCP density for mono-disperse hard spheres^{2,4,6} is commonly quoted to be 63–64%; here we physically interpret a state with this value as the ground state of frictional hard spheres characterized by a given interparticle friction coefficient. In this representation, as μ varies from zero to infinity, the RCP state changes accordingly. This approach leads to an unexpected number of states lying in an 'RCP line' from the frictionless point at $Z = 6$ to the point at $Z = 4$, as depicted in Fig. 1, demonstrating that RCP is not a unique point in the phase diagram.

Second, equation of state (5) provides the lowest volume fraction for a given Z and represents a statistical interpretation of the RLP limit depicted by the 'RLP line' in Fig. 1. We predict that to the left of this line packings either are not mechanically stable or are experimentally irreversible as discussed in refs 8, 11, 25. There is no general consensus on the value of the RLP density: different estimates have been reported, ranging from 0.55 to 0.60 (refs 4–6). The phase diagram offers a solution to this problem. Along the infinite-compactivity RLP line, the volume fraction of the RLP decreases with increasing friction from the frictionless point $(\phi, Z) = (0.634, 6)$ (ref. 21), called the 'J-point' in ref. 22, towards the limit of infinitely rough hard spheres. Indeed, experiments⁴ indicate that lower volume fractions are associated with larger coefficients of friction. We predict the lowest volume fraction to be $\phi_{\text{RLP}}^{\text{min}} = 4/(4+2\sqrt{3}) \approx 0.536$, in the limit as $\mu \rightarrow \infty$, $X \rightarrow \infty$ and $Z \rightarrow 4$ ($h_z \ll 1$). Although this is a theoretical limit, our results indicate that for $\mu > 1$ this limit can be approximately achieved. The existence of an RLP bound is an interesting prediction of the present theory. The RLP limit has been little investigated experimentally, and currently it is not known whether this limit can be reached in real systems. Our prediction is close to the lowest stable volume fraction ever reported for monodisperse spheres⁵, namely 0.550 ± 0.006 .

Third, between the two RLP and RCP limits, there are packings inside the yellow zone in Fig. 1 with finite compactivity, $0 < X < \infty$. In such cases we solve the partition function numerically to obtain $\phi(X, Z)$ along an isocompactivity line, as shown in the colour lines in Fig. 1. The compactivity X controls the probability of each state, through a Boltzmann-like factor in equation (3) (as in condensed matter physics), and characterizes the number of possible ways of rearranging a packing having a given volume and entropy, S . Thus, the limits of the most compact and least compact stable arrangements correspond to $X \rightarrow 0$ and $X \rightarrow \infty$, respectively. Between these limits, the compactivity determines the volume fraction from RCP to RLP.

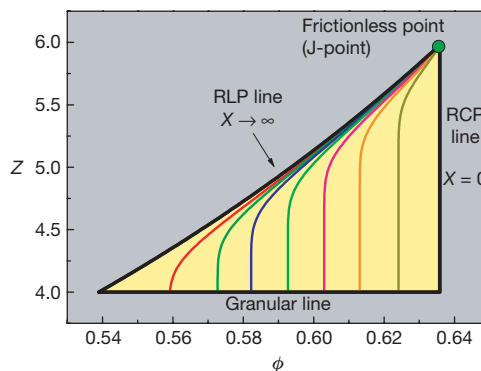


Figure 1 | Phase diagram of jamming: theory. Theoretical prediction of the statistical theory. All disordered packings lie within the yellow triangle demarcated by the RCP line, RLP line and granular line. Lines of uniform finite compactivity are in colour. Packings are forbidden in the grey area.

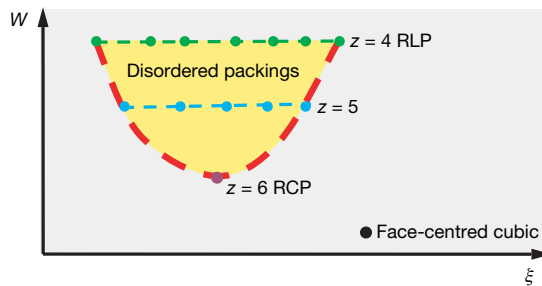


Figure 2 | Representation of the volume landscape of jammed matter (ξ, W). The multidimensional coordinate ξ represents the degrees of freedom: particle positions and rotations. Each dot represents a discrete jammed state at a given z ; those lying on a line of constant volume W share a common z value. We present the $\mu = \infty$ case. The states represent those along the granular line in Fig. 1 as the compactivity varies from $X = 0$ (ground state) to $X \rightarrow \infty$ (RLP limit). The ground state of jammed matter for this friction coefficient has $z = 6$ and the highest volume states are found for $z = 4$. For other finite values of μ , the space is delimited above by a line of constant $z = Z(\mu)$. All disordered packings lie in the yellow region of the phase space, which corresponds to the isostatic plane of hard spheres at the jamming transition where our calculations are performed. Other ordered packings, such as the face-centred cubic, have lower volume.

These results can be visualized in terms of a ‘volume landscape’ analogous to the energy landscape in glasses²⁶. Each jammed state (determined by the positions and rotations of the particles, denoted ξ , and the corresponding free volume, W) is depicted as a point in Fig. 2. The volume landscape has different levels of constant W determined by z , analogous to energy levels in hamiltonian systems. The lowest volume corresponds to the face-centred-cubic/hexagonal-close-packed structure (with $z = 12$), as conjectured by Kepler. Other lattice packings, such as the cubic lattice and tetrahedron lattice, have higher volume levels in this representation. Beyond these ordered states, the ensemble of disordered packings is identified within the yellow area in Fig. 2, corresponding to a system with infinite friction. Equation (4) indicates that the RCP corresponds to the ground state of disordered jammed matter for a given friction, which determines Z , whereas the RLP states are achieved for higher volume levels, as indicated in Fig. 2.

Further statistical characterization of the jammed structures can be obtained by solving the equations of state in the three-dimensional X - ϕ - S space, as in Fig. 3 (see Supplementary Information section V).

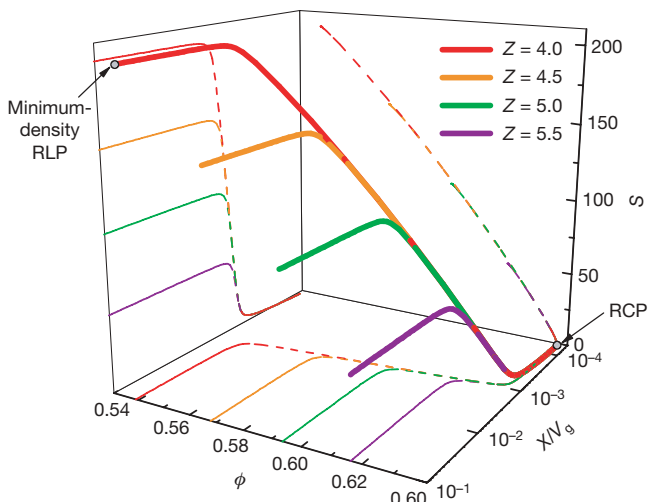


Figure 3 | Predictions of the equation of state of jammed matter in the X - ϕ - S space. Each line corresponds to a different system with Z as indicated. The projection in the X - ϕ plane qualitatively resembles the compaction curves of the experiments in refs 8, 11, 25.

Each curve in the figure corresponds to a system with a different $Z(\mu)$. The solution to the equation of state for $\phi(X)$ can be seen for different values of Z in the projection in Fig. 3. The volume fraction diminishes with increasing compactivity according to the theoretical picture of the phase diagram. The curves $\phi(X)$ qualitatively reproduce the reversible branch of compaction curves in the experiments of ref. 8 for shaken granular materials and oscillatory compression of grains²⁵, suggesting a correspondence between X and shaking amplitude. The idea is that different control parameters in experiments could be related to a state variable, and therefore might help experimentalists to describe results obtained under different protocols. For any value of Z , there is a common limit, $\phi \rightarrow \phi_{RCP}$, as $X \rightarrow 0$, giving the constant volume fraction for all the RCP states. The singular nature of the frictionless J-point is apparent from the fact that the volume fraction remains constant for any value of X , explaining why this point is the confluence of the isocompactivity lines, including RCP and RLP.

The existence of the theoretically inferred jammed states opens such predictions to experimental and computational investigation. We numerically test the predictions of the phase diagram by preparing monodisperse packings of Hertz–Mindlin spheres with friction coefficient μ at the jamming transition using previously developed methods^{21,27}. We obtain different packing states by compressing a system from an initial volume fraction ϕ_i with a compression rate Γ in a medium of viscosity (damping) η (see Supplementary Information section VIA). Although the simulations are not realistic (we do not use gravity, boundaries or a realistic protocol), they provide a way to test the main predictions of the theory. In Fig. 4 we plot the final state (ϕ, Z) reached by the system for every quadruplet $(\phi_i, \Gamma, \eta, \mu)$ at the jamming transition of vanishing stress, using a method explained in Supplementary Information section VIB. As in other non-equilibrium systems, such as glasses, the inherent path dependency of jammed matter is manifest in the fact that different packing structures can be realized using different preparation

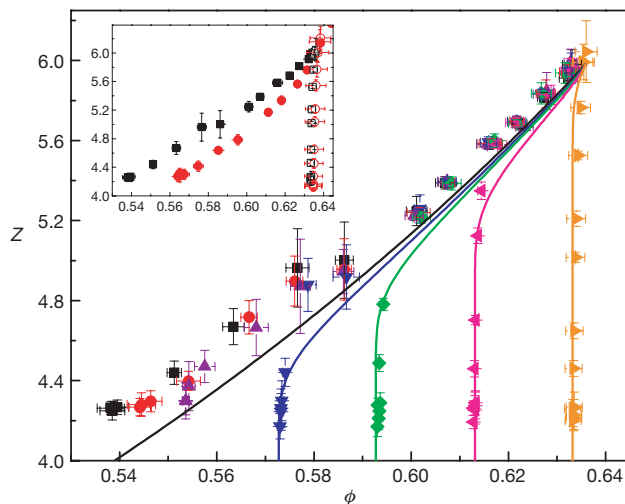


Figure 4 | Phase diagram of jamming: simulations. Numerical simulations demonstrate how to dynamically access the theoretically found states. The numerical protocol is parameterized by $(\phi_i, \Gamma, \eta, \mu)$. The main plot shows the dependence of the final jammed states (ϕ, Z) on ϕ_i for fixed $\Gamma = 10^{-7}$ and $\eta = 10^{-3}$ (except for the data plotted in orange, which is for $\eta = 10^{-4}$) and the ϕ_i values 0.40 (black), 0.53 (red), 0.55 (violet), 0.57 (blue), 0.59 (green), 0.61 (pink) and 0.63 (orange). For each ϕ_i , the different points have different values of μ (see Supplementary Fig. 10). Solid lines represent the theoretical results, with $h_z = e^{-100}$, for the following values of compactivity X (in units of $10^{-3}V_g$): infinity (black), 1.62 (blue), 1.38 (green), 1.16 (pink) and 0.88 (orange). The inset (which has the same axes as the main panel) focuses on the dependence of (ϕ, Z) on (Γ, η) for two different ϕ_i values. Filled symbols are for $\phi_i = 0.40$ and the (Γ, η) values $(10^{-7}, 10^{-3})$ (black) and $(10^{-4}, 10^{-4})$ (red). Open symbols are for $\phi_i = 0.63$ and the (Γ, η) values $(10^{-7}, 10^{-3})$ (black) and $(10^{-3}, 10^{-4})$ (red). The error bars correspond to the standard deviation over ten realizations of the packings.

protocols^{8,11,25}. Indeed, the present algorithm has analogies with recent attempts to describe jamming using ideas from the theory of mean-field spin glasses and optimization problems^{28,29}.

Changing the initial volume fraction ϕ_i produces different packings, as seen in Fig. 4. As ϕ_i increases, the final volume fraction approaches the prediction of the vertical RCP line of zero compactivity, demonstrating how to access the range of RCP states. All RCP states have approximately the same geometrical coordination number, $z \approx 6$, but differ in mechanical coordination number, with values ranging from $Z = 6$ to $Z \approx 4$, as predicted by the theory. When considering packings prepared with the smallest ϕ_i , slower compression rates (see Fig. 4 inset) or larger viscosities of the medium, we produce states with infinite compactivity along the RLP line. These results agree with the experiments of ref. 5: RLP is found for slowly deposited grains. Furthermore, packings prepared with intermediate values of ϕ_i closely follow the lines of isocompactivity shown in Fig. 4. Thus, to a reasonable approximation and for this particular protocol, we identify the density of the initial state, ϕ_i , with the compactivity of the packing, which provides a way to prepare a packing with a desired compactivity. In general, all numerically generated jammed states lie approximately within the predicted bounds of the phase diagram (see Supplementary Information section VIC for further details).

The numerical results indicate a way to test the existence of the predicted packings experimentally. By allowing the grains to settle in liquids of varying density, the speed of the particles can be varied and a systematic exploration of the jamming phase diagram can be made. Beyond the elucidation of some questions about the sphere-packing problem, other problems can now be addressed systematically using the phase diagram. These include the investigation of the criticality of the jamming transition from frictionless to frictional systems by extending the phase space to include stress; the characterization of jamming in the phase space of configurations; the problem of elasticity and Green's function; and the study of the distribution of forces, volumes and coordination numbers, to name a few. An advantage of the present formalism is that it provides a unified classification of jammed packings using which these studies could be systematically performed.

Received 3 December 2007; accepted 8 April 2008.

- Hales, T. C. The Kepler conjecture. Preprint at (<http://arxiv.org/abs/math/9811078v2>) (2002).
- Bernal, J. D. & Mason, J. Packing of spheres: co-ordination of randomly packed spheres. *Nature* **188**, 910–911 (1960).
- Behringer, R. P. & Jenkins, J. T. (eds) *Powders & Grains* 97 (Balkema, Rotterdam, 1997).
- Scott, G. D. & Kilgour, D. M. The density of random close packing of spheres. *J. Phys. D* **2**, 863–866 (1969).
- Onoda, G. Y. & Liniger, E. G. Random loose packings of uniform spheres and the dilatancy effect. *Phys. Rev. Lett.* **64**, 2727–2730 (1990).
- Berryman, J. D. Random close packing of hard spheres and disks. *Phys. Rev. A* **27**, 1053–1061 (1983).
- Edwards, S. F. & Oakeshott, R. B. S. Theory of powders. *Physica A* **157**, 1080–1090 (1989).

- Nowak, E. R., Knight, J. B., Ben-Naim, E., Jaeger, H. M. & Nagel, S. R. Density fluctuations in vibrated granular materials. *Phys. Rev. E* **57**, 1971–1982 (1998).
- Blumenfeld, R. & Edwards, S. F. Granular entropy: explicit calculations for planar assemblies. *Phys. Rev. Lett.* **90**, 114303 (2002).
- Ball, R. C. & Blumenfeld, R. Stress field in granular systems: loop forces and potential formulation. *Phys. Rev. Lett.* **88**, 115505 (2002).
- Schröter, M., Goldman, D. I. & Swinney, H. L. Stationary state volume fluctuations in a granular medium. *Phys. Rev. E* **71**, 030301(R) (2005).
- Fierro, A., Nicodemi, M., Tarzia, M., de Candia, A. & Coniglio, A. Jamming transition in granular media: A mean-field approximation and numerical simulations. *Phys. Rev. E* **71**, 061305 (2005).
- Aste, T., Saadatfar, M. & Senden, T. J. Local and global relations between the number of contacts and density in monodisperse sphere packs. *J. Stat. Mech.* P07010 (2006).
- da Cruz, F., Lechenault, F., Dauchot, O. & Bertin, E. Free volume distributions inside a bidimensional granular medium, in *Powders and Grains 2005* (eds García-Rojo, R., Herrmann, H. J. & McNamara, S.) (Balkema, Rotterdam, 2005).
- Bertin, E., Dauchot, O. & Droz, M. Definition and relevance of nonequilibrium intensive thermodynamic parameters. *Phys. Rev. Lett.* **96**, 120601 (2006).
- Ciamarra, M. P., Coniglio, A. & Nicodemi, M. Thermodynamics and statistical mechanics of dense granular media. *Phys. Rev. Lett.* **97**, 158001 (2006).
- Brujić, J., Edwards, S. F., Hopkinson, I. & Makse, H. A. Measuring distribution of interdroplet forces in a compressed emulsion system. *Physica A* **327**, 201–212 (2003).
- Torquato, S., Truskett, T. M. & Debenedetti, P. G. Is random close packing of spheres well defined? *Phys. Rev. Lett.* **84**, 2064–2067 (2000).
- Alexander, S. Amorphous solids: their structure, lattice dynamics and elasticity. *Phys. Rep.* **296**, 65–236 (1998).
- Edwards, S. F. & Grinev, D. V. Statistical mechanics of stress transmission in disordered granular arrays. *Phys. Rev. Lett.* **82**, 5397–5400 (1999).
- Makse, H. A., Johnson, D. L. & Schwartz, L. M. Packing of compressible granular materials. *Phys. Rev. Lett.* **84**, 4160–4163 (2000).
- O'Hern, C. S., Langer, S. A., Liu, A. J. & Nagel, S. R. Random packings of frictionless particles. *Phys. Rev. Lett.* **88**, 075507 (2002).
- Silbert, L. E., Ertas, D., Grest, G. S., Halsey, T. C. & Levine, D. Geometry of frictionless and frictional sphere packings. *Phys. Rev. E* **65**, 031304 (2002).
- Torquato, S. & Stillinger, F. H. Multiplicity of generation, selection, and classification procedures for jammed hard-particle packings. *J. Phys. Chem. B* **105**, 11849–11853 (2001).
- Brujić, J. et al. Granular dynamics in compaction and stress relaxation. *Phys. Rev. Lett.* **95**, 128001 (2005).
- Stillinger, F. H. A topographic view of supercooled liquids and glass formation. *Science* **267**, 1935–1939 (1995).
- Zhang, H. P. & Makse, H. A. Jamming transition in emulsions and granular materials. *Phys. Rev. E* **72**, 011301 (2005).
- Parisi, G. & Zamponi, F. The ideal glass transition of hard spheres. *J. Chem. Phys.* **123**, 144501 (2005).
- Krzakala, F. & Kurchan, J. Landscape analysis of constraint satisfaction problems. *Phys. Rev. E* **76**, 021122 (2007).

Supplementary Information is linked to the online version of the paper at www.nature.com/nature.

Acknowledgements This work is supported by the National Science Foundation, CMMT Division and the US Department of Energy, Office of Basic Energy Sciences, Geosciences Division. We are grateful to J. Brujić, A. Yupanqui and M. Makse for stimulating discussions.

Author Information Reprints and permissions information is available at www.nature.com/reprints. Correspondence and requests for materials should be addressed to H.A.M. ([hmkse@lev.cny.cuny.edu](mailto:hmakse@lev.cny.cuny.edu)).